TECHNICAL PAPER

Multi-band piezoelectric vibration energy harvester for low-frequency applications

Jaya Chandwani[1] · Rohit Somkuwar[1] · Raghavendra Deshmukh[1]

Abstract

Piezoelectric Energy Harvester (PEH) is a promising technology for harvesting energy from low frequency ambient vibrations. To generate the power from these low-frequency signals, PEH device must adapt its attributes according to respective applied input frequency range or has a wide operational frequency band. This paper presents, an experimental study of PEH providing two different modes of operation. The first working mode is a result of beams resonant frequency which is auto-tunable due to moving Centre of Gravity (CoG). The second mode of operation is mainly due to cylinders rotational and vibration motion creating impact on beams surface as well as on walls of proof mass. The device provides dual band nature for applied frequency range. The maximum power transfer is studied by varying the resistive load experimentally and FEM simulation is also carried out for the same. First working mode provides frequency band of 21–35Hz generating average power (r.m.s.) of 6μW with the optimal load of 5MΩ. Second working mode has a frequency band of 45–60 Hz with an average harvested power (r.m.s.) of 7.75μW with 2MΩ optimal load. The maximum harvested output power (r.m.s.) is 13.18μW. The effect of acceleration is studied for both working modes of the device. The frequency tuning range for the device is obtained as 46.96% for the provided band.

1 Introduction

Uninterrupted power source is a substantial need in the era of IoT and wireless sensor nodes. Without power, sensor nodes will die down causing a stoppage to the primary source of information of IoT. Though batteries provide power, their capabilities are finite and those cannot be reliable in the acute conditions. Harvesting power from the available physical energies such as solar, wind, vibrations, radiations etc. is the best solving for such dire needs. Electrostatic (Cottone et al. 2014; Madinei et al. 2016; Beeby et al. 2006), electromechanical (Jackson et al. 2015; Saadon and Sidek 2015; Jia and Seshia 2016; Li et al. 2014) and piezoelectric (Zhu et al. 2010; Klah and Najafi 2008; Challa et al. 2008; Li et al. 2011) transducers are available for energy harvesting. However, Piezoelectric Energy Harvester (PEH), due to its high power density and high voltage generation capability, is emerged as a major research field in this direction. This study mainly focused

on the use of mechanical vibrations for harvesting energy. Mechanical vibrations are generated from different man-made machines, infrastructures or any vibrating objects. To extract this mechanical energy and convert it into electrical usable energy, transducers are mounted on the vibrating platform. Vibration based PEH is a viable option in such scenario. Cantilever based structure is one of the most commonly used designs for PEH. This type of harvester provides the maximum power only at its resonance, i.e., when

$$\frac{f_{piezo}}{f_{source}} = 1 \qquad (1)$$

where, f_{piezo} is natural frequency of the device and f_{source} is input vibration frequency.

If the value of f_{source} shifts away slightly from f_{piezo}, the output power reduces drastically. Therefore, single resonant cantilever structures have limitations. However, a device with multiple resonant frequencies can achieve output power multiple of that of single cantilevered structure. As a result, researchers have started concentrating on wideband or tunable harvesters that have multiple resonant frequencies. Multi-resonant devices are made up with array based arrangement (Xue et al. 2008; Shahruz 2006;

✉ Jaya Chandwani
  jay13ch@gmail.com

1 Centre for VLSI and Nanotechnology, VNIT, Nagpur, Maharashtra, India

Meruane and Pichara 2016) or addition of non-linear structure (Miller et al. 2013; Somkuwar et al. 2018; Wu et al. 2014; Friswell et al. 2012) to the existing design. The non-linear arrangements have one or more oscillating structures that introduces a non-linearity in the device which increases the number of resonant frequencies of the harvester. In Jackson et al. (2016), a liquid filled proof mass is used for increasing bandwidth with change in CoG caused by dynamic movement of the liquid. This paper analyses dynamic behaviour by varying density and viscosity of liquid. The density of liquid has dominant effect on the performance. Liquid metal with substantially higher density is used by Jackson and Stam (2018) produces a sloshing effect when excited. In this, bandwidth is increased by 6.5 times the air-filled mass. Similar behaviour is observed in current study, where the solid cylinders impacting the walls of hollow proof mass is used for enhancing the bandwidth. In Wu et al. (2008) an adjustable screw is used for changing the CoG of complete mass. The tuning is manual by moving screw from one end to another end for changing the resonance frequency of the device. Another non-linear mechanism is reported in Andò et al. (2010) and Cottone et al. (2009), presents non-linear energy harvester based on interaction of permanent magnets used for widening the bandwidth of the device. Magnetic coupling for bistable two degree of freedom piezoelectric energy harvester is presented in Wang and Tang (2017). Here, secondary beam is attached to main energy harvesting beam providing two resonant peaks whereas magnetic coupling introduces non-linear dynamics which leads to broadening of the band.

Impedance of PEH is a time dependent entity and it varies with an externally applied frequency. To track real-time variation in the impedance, a complex circuitry is required. When harvester is connected to load, impedance matching is must for maximum power transfer. Any mismatch in the impedances reduces the power delivered to load drastically. Techniques like Maximum Power Point Tracking (MPPT) circuits (Zhang et al. 2012; Cai and Manoli 2017; Kong et al. 2010; Wang et al. 2011) are used for maximizing the power transfer. However, MPPT requires additional power to match up the impedance of the device with the load. This reduces the overall power generated by the device. Conventional energy harvesting devices have internal impedance which depends on external vibration frequency. Therefore, with a change in input frequency, the impedance of the device also changes, which further results into a reduced power transfer.

In this study, we have used a cantilever based device with hollow rectangular proof mass encapsulating two movable solid cylinders. These movable cylinders provide extra degree of freedom to the device. These adjustable degrees enables self adaptive property which is used for harvesting energy from the broad range of excitation frequencies by the device. The proposed device works in two different modes. In the first mode, self adjusting CoG plays an important role in the frequency tuning. This adjustment results in the formation of first frequency band. While, the second mode introduces non-linearity in the device and thereafter set up the second frequency band. Resistive impedance matching is carried out manually for both the bands. Resistive load of multiple resistances is connected to the device and power output tested for maximum value that defines the load for the particular band. Also, effect of acceleration on the frequency bands and the output power are studied.

2 Concept and design

The device design is based on moving mass inside a hollow rectangular proof mass. The analytical and experimental analysis is thoroughly described in Somkuwar et al. (2018). The unimorph type cantilevered structure with hollow proof mass is shown in Fig. 1. The working of the device is broadly divided into two modes explained as follows:

2.1 First working mode of PEH

Two movable cylindrical masses are enclosed within a hollow transparent rectangular proof mass. Therefore, the complete proof mass is a combination of two movable cylinders with an enclosure of hollow proof mass. The aluminium cantilever beam with commercial piezo layer attached is shown in Fig. 1. The commercial piezoelectric layer is a unimorph type cantilevered structure with piezo layer sandwiched between electrodes.

At no applied input, cylinders acquire a fixed position inside a hollow proof mass. At this stable position, centre of gravity (CoG) of each element *viz.* two movable cylinders and hollow proof mass is concentrated at its body centre whereas CoG of complete proof mass is different than individual CoG. For calculating the natural frequency, equivalent CoG of complete proof mass must be known and depends on the position of encapsulated cylinders. The working principle (Somkuwar et al. 2018) is shown in Fig. 2.

It is observed from Fig. 2 that the proof mass is divided into fixed and movable masses, i.e., hollow proof mass is fixed one and two solid metallic cylinders are movable mass. Mass of hollow proof mass is denoted by m_p and mass of cylinders 1 & 2 is denoted by m_{c1} and m_{c2}, respectively. The overall mass M of complete proof mass including movable cylinders obtained by adding all individual masses and given as,
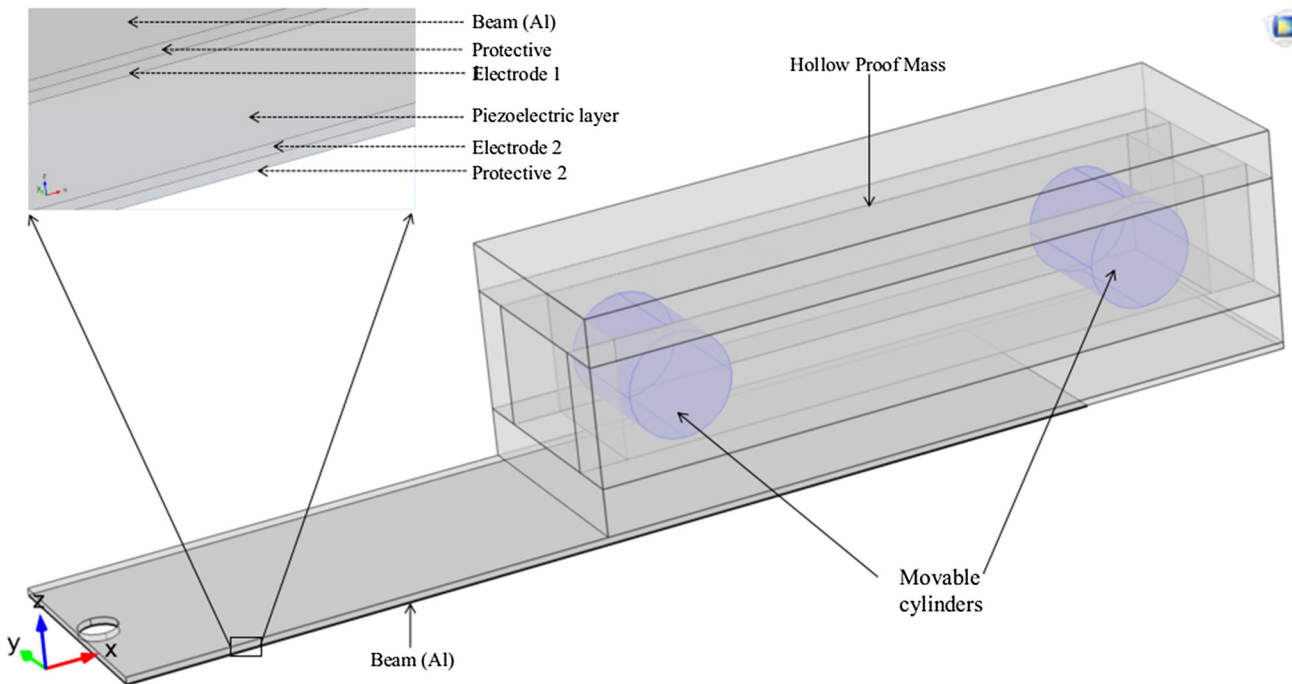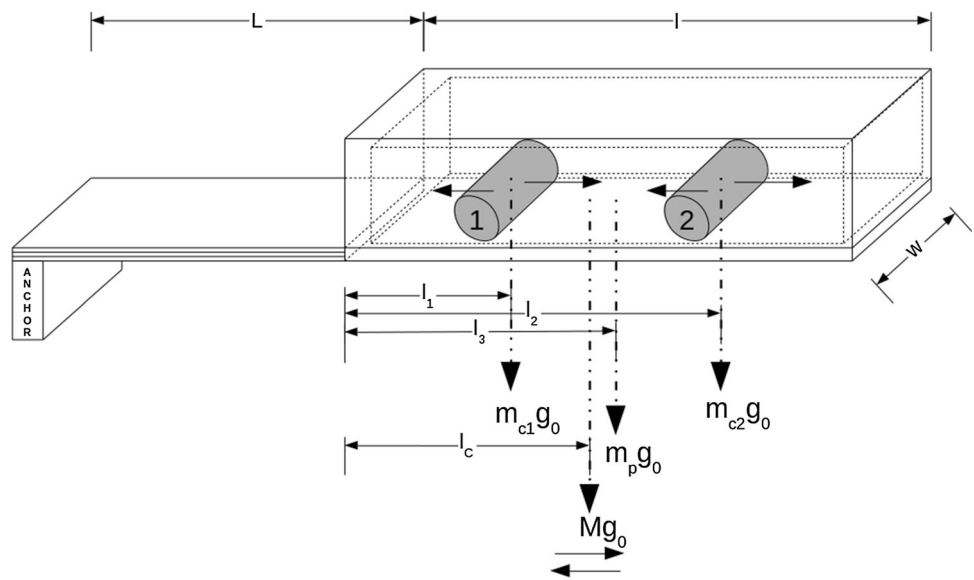
Fig. 1 Tunable energy harvester with movable cylinders

Fig. 2 Working concept of proposed design based on CoG (Somkuwar et al. 2018)

$$M = m_{c_1} + m_{c_2} + m_p \qquad (2)$$

Once, the mass of complete proof mass is obtained, the CoG can be defined as follows:

$$l_c = \left(m_{c_1} l_1 + m_{c_2} l_2 + m_p l_3 \right) / M \qquad (3)$$

where, l_c is the position of CoG of complete proof mass, M is the mass of whole proof mass, l_1, l_2 & l_3 is the position of CoG of C_1, C_2 and hollow proof mass respectively (see Fig. 2)

Resonant frequency of the beam can be approximated by applying Rayleigh's principle with uniformly distributed mass Roylance and Angell (1979) and is given by

$$\omega_n = \sqrt{\frac{EI_z}{ML^3} \frac{6\upsilon^2 + 6\upsilon + 2}{8\upsilon^4 + 14\upsilon^3 + 10.5\upsilon^2 + 4\upsilon + \frac{2}{3}}} \qquad (4)$$

where, $\upsilon = l_c/L$, l_c is the position of CoG from fixed end and L length of the beam. The Complete description with mass and CoG calculation is explained in Somkuwar et al. (2018).

The device when excited with a vibrating source, movable cylinders start moving inside the hollow proof mass. With every movement, the CoG of individual moving masses as well as complete proof-mass changes which result into a change in natural frequency of the device. Once device is excited at its natural frequency, the masses acquire unique position inside proof-mass where there is minimum potential energy Kozinsky (2009). Cylinders remain at this position until the excitation frequency changes. If frequency changes, device adapts its internal degrees of freedom with cylinders movement to acquire minimum potential energy position and hence stays in resonance for applied input frequencies. As shown in Fig. 6, for every change in excitation frequency, position of mass changes which further changes the CoG of complete proof mass, defining new natural frequency of the device.

2.2 Second working mode of PEH

When the device is excited with frequency other than beam's resonance frequency, the movement of cylinder plays an important role. This movement introduces non-ideality in the working of the device.

When the beam is not in resonance, and it is excited at higher frequency, then both cylinders occupies a fixed position near free end. At this position, these cylinders start spinning and wobbling with increased rate at that position. Here, the cylinders impacts on the beam at free end, hence stress is exerted on the piezoelectric layer which in-turn causes the increment in output voltage.

This output remains stable until the cylinders are at free end. The behaviour of cylinder is repetitive for a particular frequency band, once excitation frequency increases beyond this band, the cylinders separate from each other and the stress developed by these cylinders is drastically reduced. Both cylinders acquire two extreme ends of proof mass such that stress developed is minimized. Hence, the output voltage beyond this frequency band is lower.

The present work is purely experimental and non-ideality of the device is difficult to explain using analytical and numerical simulations. The basic equations of motion for beam and cylinders are presented in Somkuwar et al. (2018).

2.3 Electrical equivalent of piezoelectric energy harvester

The electrical equivalent of the PEH is parallel combination of resistance and capacitance Chen et al. (2017) as shown in Fig. 3. Usually, maximum power transfer is possible only when the load impedance and the internal impedance of the harvester are equal. Therefore, load impedance must match to the internal impedance of the
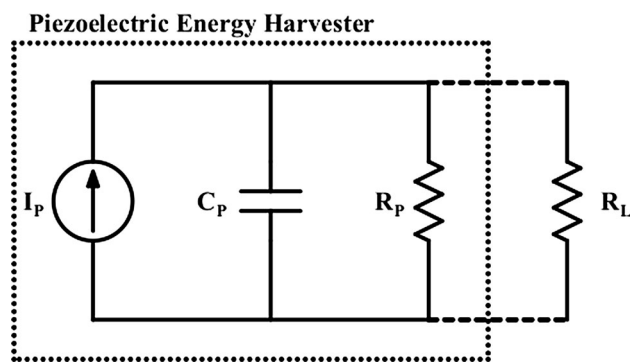
Piezoelectric Energy Harvester

Fig. 3 Electrical equivalent model for piezoelectric energy harvester

harvester. By using resistive impedance matching, the optimal load resistance ($R_{L_{opt}}$) can be calculated using Eq. 5.

$$R_{L_{opt}} = \sqrt{\frac{1}{\left(\frac{1}{R_P}\right)^2 + (2\pi f C_P)^2}} \tag{5}$$

where, f is the excitation frequency, C_P is the internal capacitance and R_P is the internal resistance of piezoelectric harvester.

Internal impedance is inversely proportional to excitation frequency, i.e., the value of optimal load decreases for higher frequencies and viceversa. As the value of R_P is large, some researchers have neglected the term $\frac{1}{R_P}$. Therefore, the Eq. 5 simplifies to

$$R_{L_{opt}} = \frac{1}{2\pi f C_P} \tag{6}$$

2.4 Device fabrication and test setup

An aluminium sheet of the prescribed dimensions is used as a main cantilever beam for the device. The hollow proof mass is assembled in a form of hollow rectangle using laser-cut acrylic sheets. The metallic cylinders are cut and encapsulated inside the hollow rectangular block. The mass of cylinders is $\approx 93\%$ of mass of hollow proof mass. The complete proof mass is then adhered to free end of cantilever beam using highly adhesive and thin double sided tape. On the other hand, commercially available piezoelectric (PVDF) sensor (TE Connectivity) is adhered to the fixed end of the cantilever beam. The fabricated device is shown in Fig. 4.

The fabricated device is tested on in-house fabricated vibration test bench. The device is mounted on vibration setup using stud tied through the hole on cantilever beam. Function generator provides the frequency input through an amplifier to the vibrating speaker. The output voltage of the
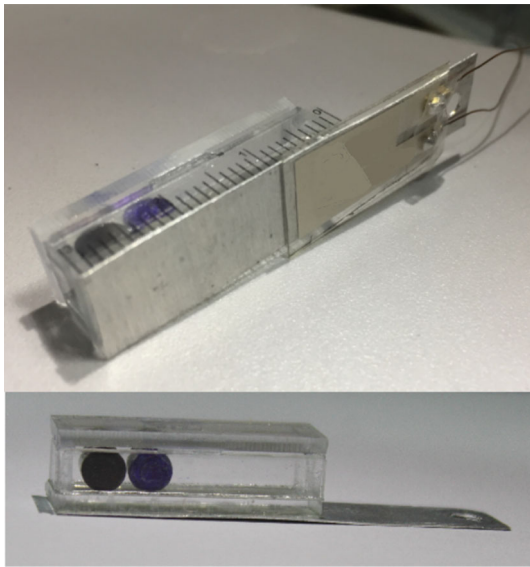
Fig. 4 Fabricated device with piezo sensor attached to it Somkuwar et al. (2018)

device is observed using real time oscilloscope by Rohde & Schwarz RTO1044 (Fig. 5).

Device properties and dimensions are provided in Tables 1 and 2 respectively.

Table 3 provides the material and dimensions of commercial piezoelectric sensor. The sensor is in the form of thin unimorph type cantilever.

3 Results and discussion

In experimentation, two distinct operating frequency bands are observed when a frequency sweep of 15–80 Hz is applied.

The basis for these bands is:

– due to the resonance of the beam and coupled motion of cylinders with beam

– due to cylinders spinning and wobbling action around its own axis at increased rate with impact on walls of proof mass and beam surface

The first frequency band of 21–35 Hz is defined as a region I, whereas 45–60 Hz is region II. Region I provides self-adjusting property where natural frequency changes with respect to change in CoG. In region II, in spite of beam's small vibrational amplitude at higher frequency, there is increase in output voltage due to cylinders increased rotating and oscillating movement at free end. For the frequencies other than region I & II (36–44 Hz), cylinders are unstable and their positions are unpredictable. Also, vibrations of the beam are reduced to miniscule. These two functional bands together increase the operating frequency range of the energy harvester (Fig. 6).

In order to validate the results of region I, firstly both cylinders are fixed at distal end (free end-away from anchor) and for this position, the resonance frequency is obtained as 19.34 Hz. Hereafter, both cylinders fixed at proximal end (fixed end near anchor) and for this position, the resonance frequency is obtained as 23.9 Hz as shown in Fig. 7. For both these conditions, the CoG is different and fixed which leads to change in resonance frequency of the device. The bandwidth for fixed mass is 4.56 Hz while for the rolling cylinders it is $\approx$ 15Hz.

3.1 Frequency band verification with frequency sweep analysis

Experimental analysis using frequency sweep operation is performed to identify the working frequency range of the device. The output voltage is measured at 5MΩ load for a frequency sweep of 15–80 Hz under base excitation of 1.4g acceleration and it is shown in Fig. 8 with its FFT. It is seen that, irrespective of the initial position of the cylinders, as the device reaches its resonance i.e. 21Hz, the CoG shifts towards the free end. The FEM simulation follows the basic equation of natural frequency i.e. $\omega = \sqrt{k/m}$

Fig. 5 Vibration test bench for the fabricated device (Somkuwar et al. 2018)
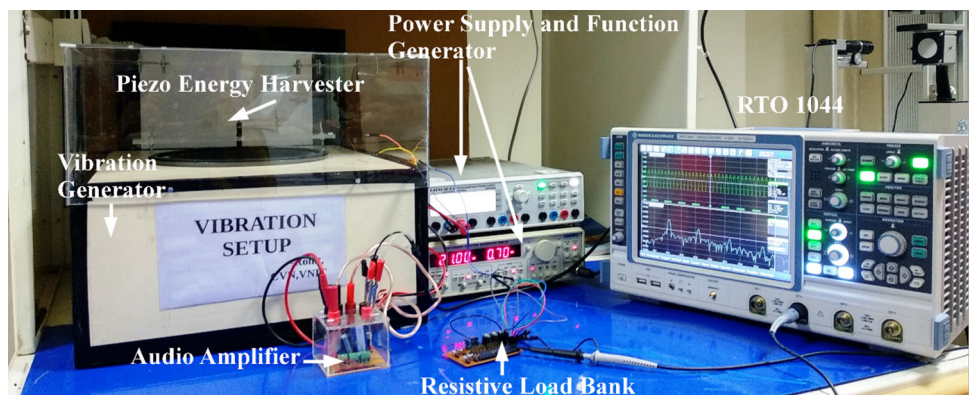
Table 1 Material properties of fabricated device

Material	Young's modulus (GPa)	Density (kg/m^3)	Poissons ratio
Aluminium (Al)	70	2700	0.33
Steel	200	7850	0.33
Acrylic plastic	3.2	1190	0.37

The material properties shown in Table 1. are taken from FEM simulator and from Material (2017)

Table 2 Dimensions of fabricated device

Beam (mm) Aluminium	Proof mass (mm) Acrylic plastic	C_1 and C_2 (mm) Steel
$50 \times 10 \times 0.28$	$2 \times (30 \times 10 \times 2)$ $2 \times (30 \times 2 \times 5)$ $2 \times (2 \times 6 \times 5)$	2.2×5

Table 3 Material and dimensions of PVDF (Polyvinylidene difluoride) piezo sensor

Layer	Material	Dimension (mm)
Piezo layer	PVDF	$40 \times 10.2 \times 0.028$
Electrodes	Silver ink	$2 \times (40 \times 10.2 \times 0.035)$
Protective layer	Acrylic plastic	$2 \times (40 \times 13 \times 0.125)$

Provided by manufacturer TE connectivity
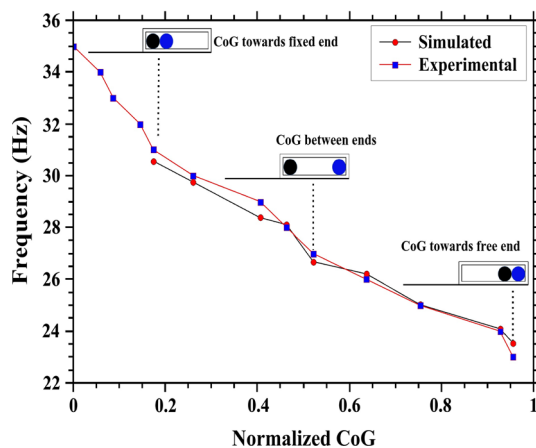
Fig. 6 Change in frequency with respect to CoG (Somkuwar et al. 2018)

providing 24.1 Hz as simulated frequency for the device. With further increase in frequency up to 35 Hz, both cylinders move towards fixed end and hence shifting the CoG towards free end. This change in CoG, changes the natural frequency as indicated in Eq. 4. This leads to resonance for complete first frequency band. For the frequency band 35–44 Hz, position of both the cylinders is
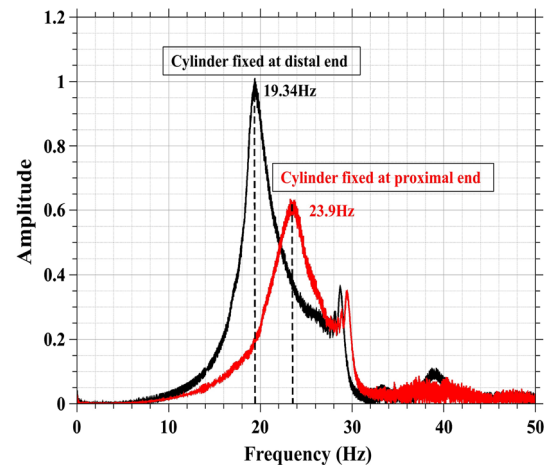
Fig. 7 Resonance frequency shift with change in CoG caused by fixed mass at distal and proximal end

uncertain. This reduces the cantilever vibration amplitude drastically, reducing the harvested energy output.

At 45–60 Hz, cylinders come towards the free end with higher rate of vibration and rotation providing the maximum output voltage as the cylinders undergo resonance in this band (region II). Herein, although the beam vibration amplitude is less, cylinders rotate in opposite direction with a high speed at the free end. This resonance of cylinders exerts stress on the piezoelectric layer resulting into the increased output voltage.

Further, increase in frequency from 61–80 Hz, cylinders again separate out and it changes the CoG of complete proof mass. In this range, cylinders acquire stable position at two opposite extremes describing CoG at the middle of proof mass.

3.2 Load dependent analysis

The open circuit voltage for the frequency of band 20–35 Hz has been analysed in Somkuwar et al. (2018). In this paper, a similar device with improved frequency range with load voltage and power is presented. If the load impedance mismatch occurs, it will lead to near zero power harvesting. Therefore, to know the optimal load impedance of the complete device is a very important and crucial job. Using the electrical equivalent model of the piezoelectric sensor,

Fig. 8 Output voltage for frequency sweep of 15–80 Hz with FFT for 5MΩ at 1.4g
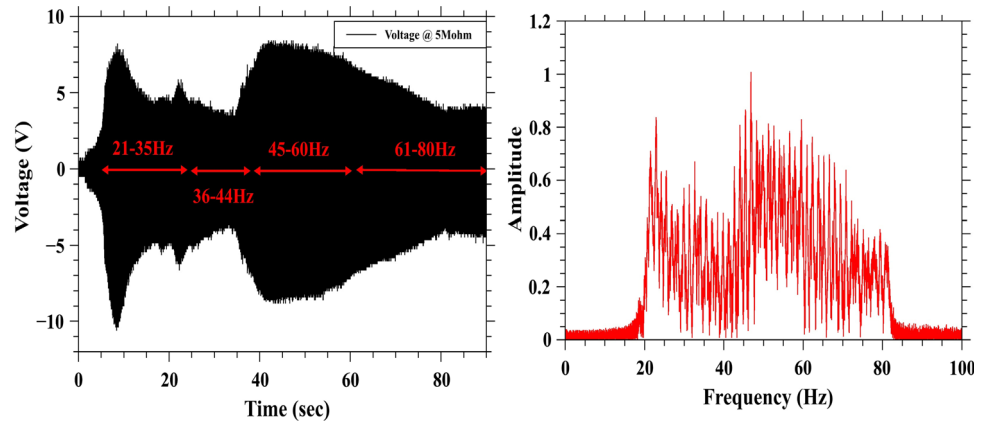
theoretically, we have calculated the optimum load impedance of the device. Initially, the resistance ($R_P = 7.65$MΩ) and capacitance ($C_P = 1.16$nF) of the complete device at steady state is measured using LCR meter (HIOKI IM3536). Theoretically calculated optimal load for region I and region II are 4.96MΩ and 2.53MΩ respectively. The capacitance value observed as 1.38nF and invariant with respect to excitation frequency. Hence, for maximum power harvesting only resistance value needs to be optimized.

The output voltage(r.m.s.) with various excitaion frequencies for different acceleratons is measured and power(r.m.s.) is evaluated for applied external resistance R_L through relation

$$P = \frac{V^2}{R_L} \tag{7}$$

Output power is measured for the frequency range of 15–80 Hz with varying load from 1MΩ to 20MΩ taken from resistive load bank under base excitation of 1.4g.
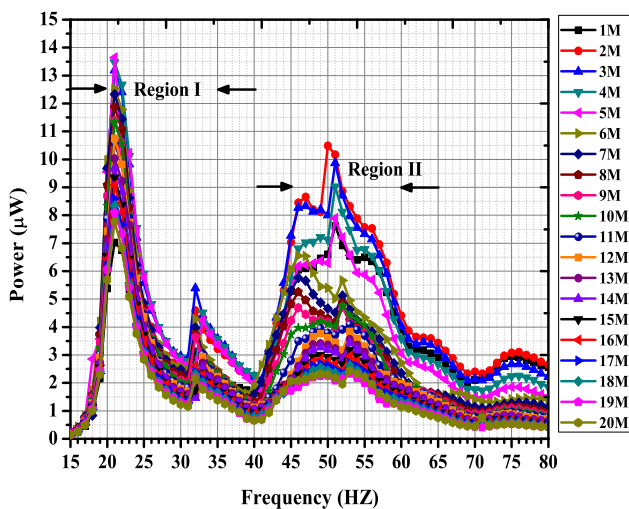

**Fig. 9** Output r.m.s Power versus load resistances under 1.4g base excitation

Fig. 9 depicts that the proposed device has two distinct frequency bands compared to conventional unimorph type cantilever device which has only one resonant frequency. This is observed due to the novel design of PEH which incorporates coupled motion of beam and cylinders inside the proof mass. The optimal load value of 5MΩ is obtained for region I. The peak obtained in region I at 21 Hz is the result of resonance of the beam. The maximum power is measured 13.18μW in this region. The load value of 2MΩ is found to be the optimal value in region II. At this load, the maximum power measured is 10.54μW at 51 Hz. The variation of optimal load for these two regions can be explained by the influence of excitation frequency. In order to get maximum power from harvester, load resistance is required to match with the source resistance. The obtained optimal load values for these two regions are found approximately equal to theoretically calculated load values using Eq. 5. Experimentally, it is verified that, as the frequency of excitation increases, the optimal load value decreases from 5MΩ to 2MΩ for region I to region II respectively as seen in Fig. 10.

Load dependent response is shown in Fig. 11 for region I using FEM tool (Comsol). The resonance is obtained at 24.1 Hz for the simulated device. For the device, maximum power observed at 5.62MΩ using FEM.

The amplitude of power is increased with an increase in acceleration as shown in Fig. 12a. The region II between 45–60 Hz shows flat response for 0.6–0.8 g because the energy provided by external excitation source is not sufficient for cylinders to provide the necessary impact on piezoelectric layer. However, at 1–1.4 g, the cylinders get excited and they start vibrating and rotating with higher amplitude that causes increased stress on piezoelectric layer resulting in a higher output power. The increment in power is attributed to large strain developed in piezoelectric layer as a result of pressure exerted by vibrating cylinders. In Fig. 12b, it is evident that there is an increase in bandwidth with an increase in acceleration as the
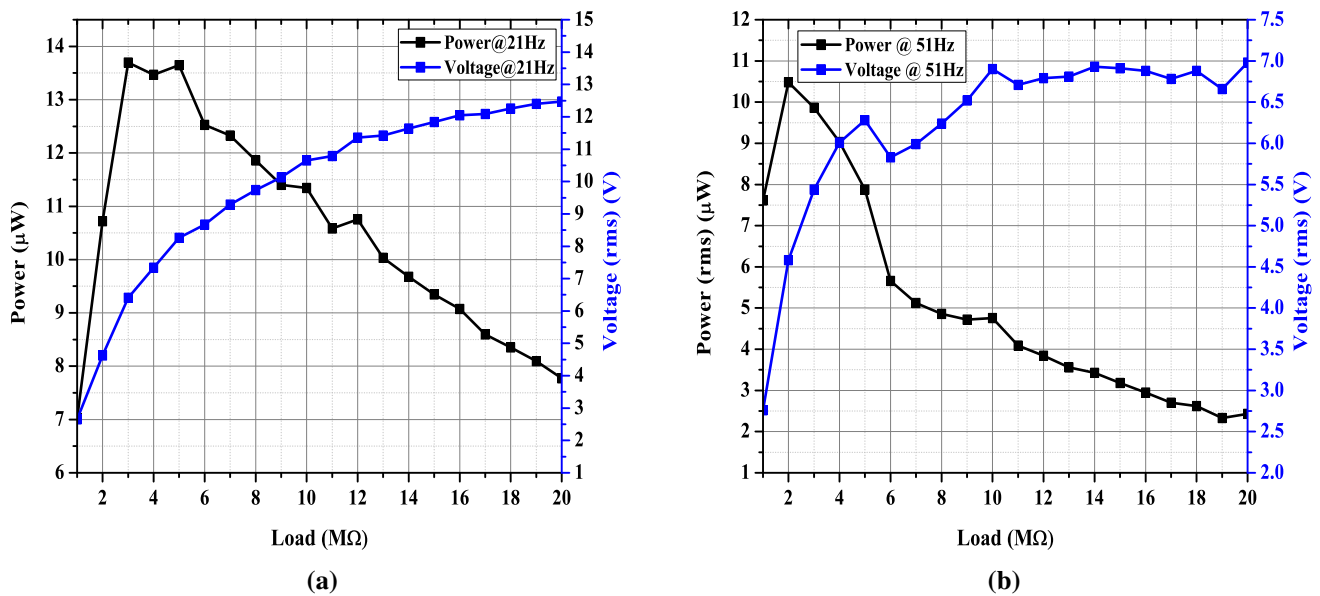
Fig. 10 Maximum r.m.s Power and voltage versus Load at **a** 21 Hz and **b** 51 Hz with 1.4g acceleration
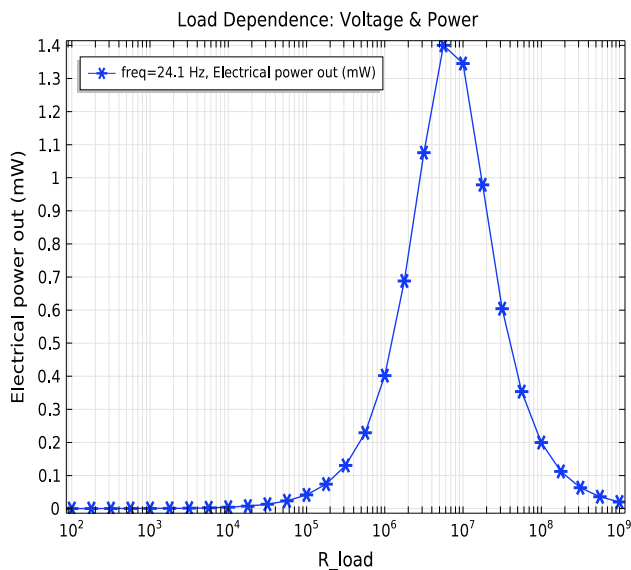
Fig. 11 Simulated load versus power for region I

dynamic non-linear movement of cylinder increases correspondingly.

The voltage and power versus acceleration behaviour of the device is depicted in Fig. 13. The maximum output power in each region is used for studying the effect of acceleration on the harvested power. As illustrated in Fig. 13a, for region I at 21 Hz the output power linearly increases with respect to acceleration as device is in the resonance mode. For region II at 51 Hz, the cylinders occupy position near free end and start vibrating with maximum amplitude. Anomalous behaviour of device results in region II as shown in Fig. 13b. The rate of

increment in output power is higher over 1g acceleration compared to that of at 0.6–1 g. Probable reason behind this is the amplitude and speed of vibration of cylinder inside proof mass is higher for 1 g acceleration and the above. The effective stiffness of the beam increases with acceleration which increases stress on the beam and the output power is increased.

3.3 Effect of ratio of mass of cylinders to hollow proof mass on bandwidth

In this part of the experiment, effect of the ratio of mass of cylinders to the hollow proof mass on bandwidth of energy harvester is studied. Here, the hollow proof mass is kept constant and mass of cylinders are changed by using metals of different densities keeping the dimensions same. The ratio of mass of hollow proof-mass to cylinders with their respective bandwidth is tabulated in Table 4. Three different materials viz. Steel (7850 kg/m³), Copper (8960 kg/m³) and Tungsten (19300 kg/m³) are used for cylinders. Experimental results show that increase in mass ratio leads to decrease in bandwidth. Hypothesis behind this is that, experimentally it is observed that with increase in the mass of the cylinders by keeping the physical parameters of beam and the acceleration of excitation constant, the dynamic movement of cylinders lessens. This is probably because of the dynamic force acting on the cylinders to push them to minimum potential energy position is insufficient due to increased mass of cylinders. This restricted movement of cylinders reduces variation in COG leading to shrinking of bandwidth. Thus, if we decrease the density of cylinders, the bandwidth increases.
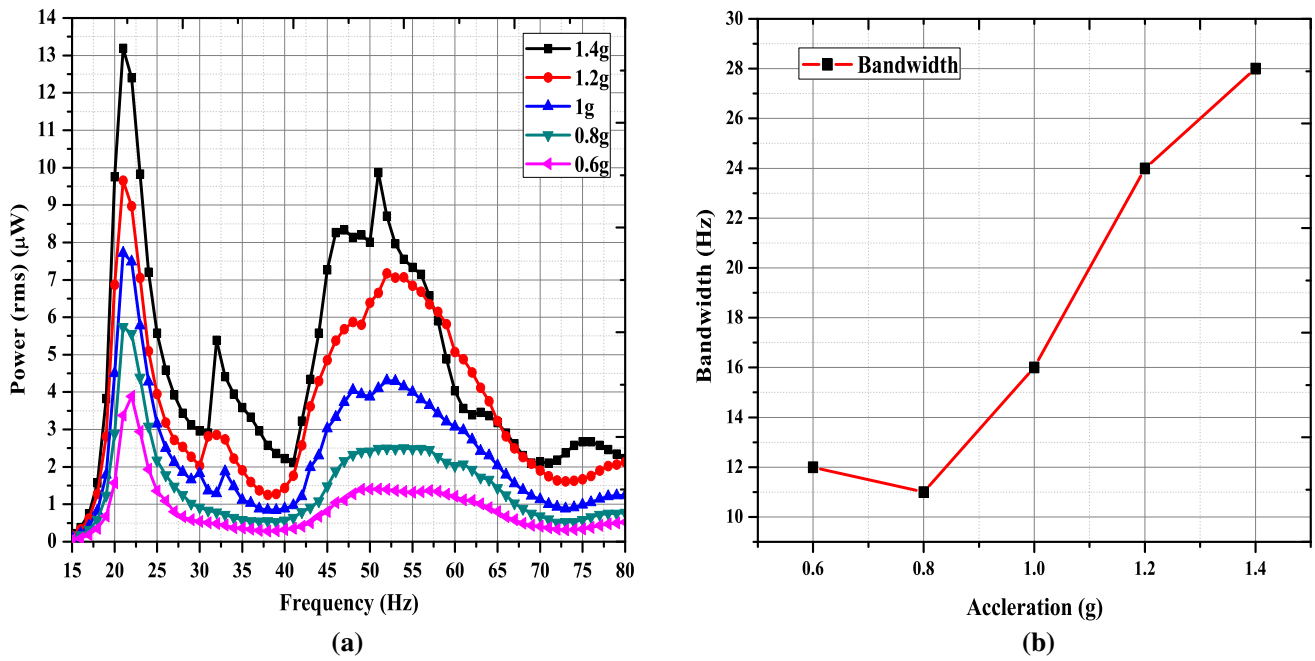
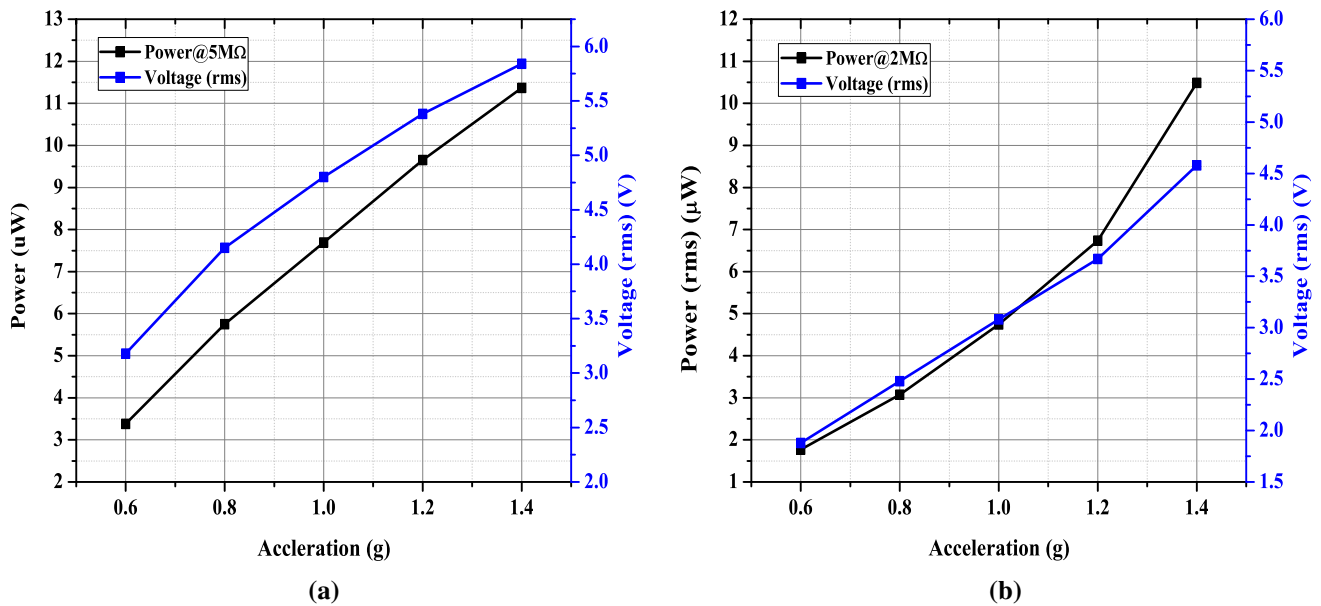**Fig. 12** **a** Frequency versus Power (rms) at various acceleration. **b** Effect of acceleration on bandwidth

Fig. 13 Maximum r.m.s power and voltage versus acceleration at **a** 21 Hz and **b** 51 Hz

Table 4 Bandwidth with respect to cylinder materials

Material	Mass (g)	Density (kg/m³)	Mass ratio	%Bandwidth
Acrylic	2.187	1190	–	–
Steel	2.037	7850	93.14%	39.23%
Copper	2.323	8960	106.2%	31.25%
Tungsten	3.807	19300	174.07%	30.29%

However, below certain density of cylinders their impact on the walls of proof-mass decreases resulting in lesser stress induced in beam leading to narrower bandwidth. Therefore, an optimization for mass ratio has to be studied. Also, non-linear coupled motion of beam and cylinders, and surface roughness play an important role for this change in the bandwidth with respect to mass of cylinders.

4 Conclusion

In this paper, experimental power analysis of non-linear PEH is presented. The prototype is designed and experimentally verified using in-house vibration test setup. The proposed PEH works in two regions of operation. The first region is a result of change in resonant frequency of the device with change in CoG of proof mass. The second region of operation is due to non-linearity introduced in the device with rotating and vibrating motion of cylinders creating an impact inside hallow proof mass. It is noteworthy that, optimal resistance values for maximum power in both regions are different. Therefore, only two resistances are sufficient to harvest maximum power from these two regions. The optimal load for region I and II are calculated analytically and those are validated with the experimental results. The maximum output power of 13.18 μW is obtained at 5 MΩ for region I. Similarly, the maximum power of 10.54 μW is harvested using 2 MΩ load for region II. The cylinder positions are undetermined between first and second working mode of the device. The frequency tuning range for the device is obtained as 46.96% for the provided band. Effect of ratio of mass of cylinders to hollow proof mass on bandwidth is studied.

In future, auto switching of optimal resistance for two regions and its effect on output power can be carried out. Also, the parameters affecting the number of operating frequency bands and the overall bandwidth of the device can be analyzed. Strategies to increase the bandwidth with maximized harvested power can be thoroughly researched out and thereafter those can be realized in the proposed device. Efforts can be made to make the bandwidth broad by decreasing the difference between two bands.

References

Andò B, Baglio S, Trigona C, Dumas N, Latorre L, Nouet P (2010) Nonlinear mechanism in MEMS devices for energy harvesting applications. J Micromech Microeng 20(1–12):125020

Beeby SP, Tudor MJ, White N (2006) Energy harvesting vibration sources for microsystems applications. Measure Sci Technol 17:R175–R195

Cai Y, Manoli Y (2017) A piezoelectric energy harvester interface circuit with adaptive conjugate impedance matching, self-startup and 71 % broader bandwidth. In: ESSCIRC 2017—43rd IEEE European Solid State Circuits Conference, pp 119–122

Challa VR, Prasad MG, Shi Y, Fisher FT (2008) A vibration energy harvesting device with bidirectional resonance frequency tunability. Smart Mater Struct 17(1–10):015035

Chen N, Wei T, Jung HJ, Lee S (2017) Quick self-start and minimum power-loss management circuit for impact-type micro wind piezoelectric energy harvesters. Sens Actuators A Phys 263:23–29

Cottone F, Vocca H, Gammaitoni L (2009) Nonlinear energy harvesting. Phys Rev Lett 102(1–4):080601

Cottone F, Basset P, Marty F, Galayko D, Gammaitoni L, Bourouina T (2014) Electrostatic generator with free micro-ball and elasticstoppers for low-frequency vibration harvesting. In: MEMS 2014, SanFrancisco, CA, USA, pp 385–388

Friswell MI, Ali SF, Bilgen O, Adhikari S, Lees AW, Litak G (2012) Non-linear piezoelectric vibration energy harvesting from a vertical cantilever beam with tip mass. J Intell Mater Syst Struct 23(13):1505–1521

Jackson N, Stam F (2018) Sloshing liquid-metal mass for widening the bandwidth of a vibration energy harvester. Sens Actuators A Phys 284:17–21

Jackson N, Stam F, Olszewski O, Doyle H, Quinn A, Mathewson A (2016) Widening the bandwidth of vibration energy harvesters using a liquid-based non-uniform load distribution. Sens Actuators A Phys 246:170–179

Jackson N, Stam F, Olszewski OZ, Houlihan R, Mathewson A (2015) Broadening the bandwidth of piezoelectric energy harvesters using liquid filled mass. Procedia Eng 120:328–332

Jia Y, Seshia AA (2016) Power Optimization by Mass Tuning for MEMS Piezoelectric Cantilever Vibration Energy Harvesting. J Microelectromech Syst 25(1):1–10

Klah H, Najafi K (2008) Energy Scavenging From Low-Frequency Vibrations by Using Frequency Up-Conversion for Wireless Sensor Applications. IEEE Sens J 8(3):261–268

Kong N, Ha DS, Erturk A, Inman DJ (2010) Resistive impedance matching circuit for piezoelectric energy harvesting. J Intell Mater Syst Struct 21:1293–1302

Kozinsky I (2009) Study of passive self-tuning resonator for broadband power harvesting. PowerMEMS 2009, Washington DC, USA, pp 388–391

Li H, Tian C, Deng ZD (2014) Energy harvesting from low frequency applications using piezoelectric materials. Appl Phys Rev 1(1–20):041301

Li M, Wen Y, Li P, Yang J (2011) A magnetostrictive/piezoelectric laminate transducer based vibration energy harvester with resonance frequency tunability. SENSORS, 2011 IEEE, Limerick, 2011, pp 1768–1771

Madinei H, Khodaparast HH, Adhikari S, Friswell MI (2016) Design of MEMS piezoelectric harvesters with electrostatically adjustable resonance frequency. Mech Syst Signal Process 81:360–374

MEMSnet, Materials (2017) A MEMS Clearinghouse® and information portal for the MEMS and Nanotechnology community. https://www.memsnet.org/material/. Accessed 24 Aug 2017 (Online)

Meruane V, Pichara K (2016) A broadband vibration-based energy harvester using an array of piezoelectric beams connected by springs. Shock Vib 2016:1–13

Miller LM, Pillatsch P, Halvorsen E, Wright PK, Yeatman EM, Holmes AS (2013) Experimental passive self-tuning behavior of a beam resonator with sliding proof mass. J Sound Vib 332(26):7142–7152

Roylance LM, Angell JB (1979) A batch fabricated silicon accelerometer. IEEE Trans Electron Devices ED–26(12):1911–1917

Saadon S, Sidek O (2015) Micro-electro-mechanical system (MEMS)-based piezoelectric energy harvester for ambient vibrations. Procedia Soc Behav Sci 195:2353–2362

Shahruz SM (2006) Design of mechanical band-pass filters for energy scavenging. J Sound Vib 292:987–998

Somkuwar R, Chandwani J, Deshmukh R (2018) Wideband auto-tunable vibration energy harvester using change in centre of gravity. Microsyst Technol 24:3033–3044. https://doi.org/10.1007/s00542-018-3846-x

Wang H, Shan X, Xie T, Fang M (2011) Analyses of impedance matching for piezoelectric energy harvester with a resistive circuit. Proc 2011 Int Confer Electr Mech Eng Inform Technol EMEIT 2011 4(1):1679–1683

Wang H, Tang L (2017) Modeling and experiment of bistable two-degree-of-freedom energy harvester with magnetic coupling. Mech Syst Signal Process 86:29–39

Wu H, Tang L, Yang Y, Soh CK (2014) Development of a broadband nonlinear two-degree-of-freedom piezoelectric energy harvester. J Intell Mater Syst Struct 25(14):1875–1889

Wu X, Lin J, Kato S, Zhang K, Ren T, Liu L (2008) A frequency adjustable vibration energy harvester. In: Proc. PowerMEMS 2008+ microEMS2008, Sendai, Japan, 9–12 November 2008, pp 245–248

Xue H, Hu Y, Wang Q (2008) Broadband piezoelectric energy harvesting devices using multiple bimorphs with different operating frequencies. IEEE Trans Ultrason Ferroelectr Freq Control 55(9):2104–2108

Zhang L, Zheng G, Li J (2012) Active piezoelectric energy harvester based on impedance matching. In: Proceeding of the IEEE International Conference on Automation and Logistics Zhengzhou, China, pp 131–135

Zhu D, Tudor MJ, Beeby SP (2010) Strategies for increasing the operating frequency range of vibration energy harvesters: a review. Measure Sci Technol 21(1–29):022001